



A new predictive dynamic model describing the effect of the ambient temperature and the convective heat transfer coefficient on bacterial growth

Hana Ben Yaghlene, Ivan Leguérinel, Moktar Hamdi, Pierre Mafart

► To cite this version:

Hana Ben Yaghlene, Ivan Leguérinel, Moktar Hamdi, Pierre Mafart. A new predictive dynamic model describing the effect of the ambient temperature and the convective heat transfer coefficient on bacterial growth. *International Journal of Food Microbiology*, 2009, 133 (1-2), pp.48-61. 10.1016/j.ijfoodmicro.2009.04.014 . hal-00553650

HAL Id: hal-00553650

<https://hal.univ-brest.fr/hal-00553650>

Submitted on 9 Jan 2012

HAL is a multi-disciplinary open access archive for the deposit and dissemination of scientific research documents, whether they are published or not. The documents may come from teaching and research institutions in France or abroad, or from public or private research centers.

L'archive ouverte pluridisciplinaire **HAL**, est destinée au dépôt et à la diffusion de documents scientifiques de niveau recherche, publiés ou non, émanant des établissements d'enseignement et de recherche français ou étrangers, des laboratoires publics ou privés.

A new predictive dynamic model describing the effect of the ambient temperature and the convective heat transfer coefficient on bacterial growth

H. Ben Yaghlene^{a,b*}, I. Leguerinel^a, M. Hamdi^b, P. Mafart^a

^a: Université Européenne de Bretagne, EA3882, Laboratoire Universitaire de Biodiversité et Ecologie Microbienne, IFR148 ScInBioS, Université de Bretagne Occidentale, 6 rue de l'université, F29334 Quimper, Cedex, France

^b: Laboratoire d'Ecologie et de Technologie Microbienne, Institut National des Sciences Appliquées et de Technologie (INSAT), 2 Boulevard de la terre, B.P. 676, 1080 Tunis, Tunisie

*Corresponding author: LUBEM, UBO, 6 rue de l'Université, F29334, Quimper Cedex, France. Tel.: +33 2 98 90 02 27; Fax: +33 2 98 90 85 44

E mail address: hana.benyaghlene@univ-brest.fr

Abstract

In this study, predictive microbiology and food engineering were combined in order to develop a new analytical model predicting the bacterial growth under dynamic temperature conditions. The proposed model associates a simplified primary bacterial growth model without lag, the secondary Ratkowsky “square root” model and a simplified two-parameter heat transfer model regarding an infinite slab. The model takes into consideration the product thickness, its thermal properties, the ambient air temperature, the convective heat transfer coefficient and the growth parameters of the micro organism of concern. For the validation of the overall model, five different combinations of ambient air temperature (ranging from 8 °C to 12 °C), product thickness (ranging from 1 cm to 6 cm) and convective heat transfer coefficient (ranging from 8 W/(m².K) to 60 W/(m².K)) were tested during a cooling

procedure. Moreover, three different ambient air temperature scenarios assuming alternated cooling and heating stages, drawn from real refrigerated food processes, were tested. General agreement between predicted and observed bacterial growth was obtained and less than 5% of the experimental data fell outside the 95 percent confidence bands estimated by the bootstrap percentile method, at all the tested conditions. Accordingly, the overall model was successfully validated for isothermal and dynamic refrigeration cycles allowing for temperature dynamic changes at the centre and at the surface of the product. The major impact of the convective heat transfer coefficient and the product thickness on bacterial growth during the product cooling was demonstrated. For instance, the time needed for the same level of bacterial growth to be reached at the product's half thickness was estimated to be 5 and 16.5 h at low and high convection level, respectively. Moreover, simulation results demonstrated that the predicted bacterial growth at the air ambient temperature cannot be assumed to be equivalent to the bacterial growth occurring at the product's surface or centre when convection heat transfer is taken into account. Our results indicate that combining food engineering and predictive microbiology models is an interesting approach providing very useful tools for food safety and process optimisation.

Key words:

Predictive microbiology; Heat transfer; Dynamic models; Bacterial growth; Cooling; Heating.

46 Nomenclature

47

A	Transfer area (m^2)
Bi	Biot number
E	Product thickness (m)
f^*	Thermal proliferation value
Fo	Fourier number
h	Convective heat transfer coefficient ($\text{W}/(\text{m}^2.\text{K})$)
j	Lag factor for reduced temperature profile
k	Slope of the linear portion of the semi-logarithmic plot of reduced temperature vs time.
l	Characteristic dimension (m)
N	Microbial cell density at time t (CFU/mL)
N_0	Initial microbial cell density (CFU/mL)
O	Observed microbial cell density (\log_{10} CFU/mL)
OD	Microbial optical density at time t
OD_0	Initial microbial optical density
P	Predicted microbial cell density (\log_{10} CFU/mL)
t	Time (s)
T	Temperature of the product ($^{\circ}\text{C}$)
T_{eq}	Equivalent temperature
T_{min}	Temperature below which no microbial growth occurs ($^{\circ}\text{C}$)
T_{opt}	Temperature at which the microbial growth is optimal ($^{\circ}\text{C}$)
T_0	Initial product temperature ($^{\circ}\text{C}$)
T_{∞}	Ambient temperature ($^{\circ}\text{C}$)
x	Distance from the centre (m)
x_{max}	Half-thickness for an infinite slab (m)
α	Thermal diffusivity of the product (m^2/s)
Γ	Overall gamma function
γ	Thermal gamma function
λ	Thermal conductivity of the product ($\text{W}/(\text{m.K})$)
μ	Specific microbial growth rate (h^{-1})
μ_{opt}	Optimal specific microbial growth rate (h^{-1})
φ	First root of $\cot \varphi = \varphi / Bi$
φ_n	Roots of $\cot \varphi = \varphi / Bi$

48

1. Introduction

Predictive food microbiology involves knowledge of microbial growth responses to environmental factors expressed in quantitative terms by mathematical equations (models) (McMeekin et al., 1997). It is generally agreed that the most important environmental factor that affects bacterial growth in food is temperature. This factor is constantly changing during processing, storage and distribution of food products (Fujikawa et al., 2004). At the same time, control organizations propose stringent requirements regarding monitoring of the internal temperature of products being processed. For instance, according to the United States Department of Agriculture, the allowable growth of *Clostridium perfringens* during the cooling of certain meat and poultry products should be limited to 1 log (U.S.D.A, 1999). In the case of cured products, the guidelines recommend that products' internal temperature should be reduced from 54.4 °C to 26.6 °C in less than 5 h, and from 26.6 °C to 7.2 °C in the next 10 h (15 h total cooling time).

Predictive microbiology is a useful tool for assessing and controlling food safety particularly when models are able to cope with dynamic conditions such as changing temperatures. Numerous published models, reported in Table 1, have dealt with the prediction of bacterial growth under dynamic temperature conditions. Generally, these works were based on predictive models corresponding to isothermal bacterial growths which were modified in order to consider the effect of temperature changes. These studies primarily aimed at assessing the feasibility of predicting the bacterial growth at changing temperature. Indeed, predicting bacterial growth under dynamic conditions has been shown to be possible via the dynamic transformation of existing static models. According to the authors of the cited studies (Table 1), the models' predictions agreed well with experimental results after temperature changes.

73 Nevertheless, the considered scenarios of changing temperatures within bacterial models were
74 various. In some cases, typical temperature profiles were considered either by the use of
75 hypothetical ones or by the adoption of real temperature scenarios recorded while the studied
76 products had been processed. In other cases, temperature profiles were simulated from heat
77 transfer models. Mathematical models that integrate effectively heat transfer phenomena and
78 dynamic bacterial growth relationships are scarce (Amezquita et al., 2005; de Jong et al.,
79 2005; Zwietering and Hasting, 1997). Armitage (1997) derived the temperature histories for
80 the deep leg and leg surface of a lamb carcass by using finite element models for dealing with
81 regular shapes. Temperature function integration technique (TFI) was applied to the
82 calculated temperature histories of five different cooling processes to simulate *Escherichia*
83 *coli* growth on the leg surface of each carcass during aging. TFI technique was previously
84 introduced by Gill and Harrison (1985). Data related to the growth of six strains of *E. coli*
85 isolated from commercially packed livers were fitted according to the Ratkowsky model
86 (Ratkowsky et al., 1982) linking the growth rate to temperature. Total growth was obtained by
87 summation of partial growth calculated within sequential 3.75-min periods from the growth
88 rate for the average temperature within each period. Estimated bacterial growth during offals
89 cooling (cooling profiles were directly recorded on several offals being chilled) agreed well
90 with observed data with *E. coli*. Bellara et al. (2000) experimentally validated bacterial
91 growth modelling involving a heat transfer model of temperature fluctuations within a solid
92 object. From data related to *E. coli* W3110 growth in agar, a model was set up describing
93 bacterial growth as a function of temperature. This was then used in conjunction with a finite
94 difference heat transfer model describing temperature change in a cylinder in order to
95 calculate the bacterial growth that occurs in agar gel inside a cylindrical glass vessel under
96 conduction cooling. Excellent agreement was found between model simulations and
97 experimental data. Alavi et al. (2001) determined the growth characteristics of *Listeria*

monocytogenes in sterilized whole milk. The parameter values of the Baranyi dynamic growth model (Baranyi et al., 1995) were determined. Finite element software, ANSYS, was implemented to determine temperature distributions in milk cartons subject to a time-varying ambient temperature profile. The space-time-temperature data were input to the Baranyi dynamic growth model, to predict the microbial population density distribution and the average population density in the milk carton. Amezcuita et al. (2005) developed a computer simulation scheme to analyze heat transfer phenomena and temperature-dependent *C. perfringens* growth during cooling of cooked boneless cured ham. The temperature history of ham was predicted from a finite element heat diffusion model. For *C. perfringens* growth, a dynamic model was developed from the Baranyi's nonautonomous differential equation (Baranyi and Roberts, 1994). The bacterium's growth model was integrated into the computer program taking predicted temperature histories as input values. Validation of the model predictions considered three different time-temperature cooling histories from 54.4 °C to 7.2 °C of the geometrical centre of a large cooked boneless ham. In a further work (Corradini et al., 2006), the same data were fitted with the ad hoc empirical models in order to define the three parameters temperature dependence of the modified version of the logistic primary model. The continuous rate equation was solved incrementally by a numerical procedure implemented in general purpose software. In both Amezcuita et al. (2005) and Corradini et al. (2006) works, predicted *C. perfringens* growth curves obtained from dynamic modelling showed good agreement with observed results for the tested cooling scenarios. The integrated modelling approach for predicting microbial behaviour during processing was reviewed by Lebert and Lebert (2006).

Combination of predictive microbiology and food engineering allows both the assessment of a process in relation to risk and its optimisation (Mafart, 2005). In spite of all the advances made in modelling microbial growth, proposing and improving new overall models which

combine predictive microbiology and heat transfer phenomena is an obvious necessity. The more simple the proposed models and the more realistic the considered conditions are, the easiest is their implementation to food processes.

In the present study, we aimed to develop a new analytical model combining bacterial growth prediction and food engineering. Our goal was for the overall model to be simple and robust, with minimum involved parameters, and to integrate the process conditions. The proposed model is the association of three equations: a simplified primary model consisting of a simple exponential growth equation without lag time, the Ratkowsky “square root” model linking the specific growth rate to temperature (Ratkowsky et al., 1982), and a simplified two-parameter heat transfer model regarding an infinite slab. While classical models assume that ambient temperature is immediately reached at the growth medium, this work takes into account, not only the air temperature, but also the thickness of the medium, its thermal properties and the convective heat transfer coefficient. In addition, the proposed model may be easily implemented to various micro organisms having known growth parameters.

2. Development of the model

2.1. Heat transfer modelling

All cooling processes for solid materials exhibit similar behaviour. After an initial ‘lag’, the reduced temperature at the thermal centre of the food item decreases exponentially. The linear portion of the cooling curve (obtained by plotting, on semi-logarithmic axes, the reduced temperature $(T_{\infty} - T)/(T_{\infty} - T_0)$ versus time (Becker and Fricke, 2004), see Fig. A1 in the appendix) can typically be described by the simplified linear asymptotic form of the general heat transfer model, valid for Fourier number $Fo \geq 0.2$ with $Fo = \alpha \cdot t / l^2$ where α is thermal diffusivity of the product, l is the characteristic dimension of the product, T is the local temperature of the product at the time t , T_0 is the initial temperature of the product, T_{∞} is the

cooling medium temperature (pulsed air). Consequently, the heating or cooling kinetic is expressed as follows:

$$T = T_{\infty} (1 - je^{-kt}) + T_0 je^{-kt} \quad (1)$$

Where j is the lag factor and k is the slope of the linear portion of the semi-logarithmic plot of reduced temperature *vs* time. The value of the parameter k depends upon the product shape, l , α and the Biot number $Bi = hl/\lambda$, where h is the convective heat transfer coefficient between the product surface area and the ambient air and λ is the thermal conductivity of the product. A low Biot number ($Bi < 0.1$) indicates that the internal resistance to heat transfer is negligible, and thus, the temperature within the object is uniform at any given instant in time while the external thermal resistance can be neglected for $Bi > 40$ (Mafart, 1997).

The governing differential equation for infinite slab is given as follows with the initial (uniform distribution of temperature) and boundary condition (surface convection):

$$\frac{\partial T}{\partial t} = \alpha \frac{\partial^2 T}{\partial x^2} \quad (2)$$

where x is distance from the centre. For initial condition of uniform temperature and boundary conditions of central symmetry and convective heat transfer at the surface, solution for Eq. (2) is supplied by the infinite series given by Carslaw and Jaeger (1986) (see Eq. (20) in the appendix). It is a general knowledge that use of the first term of this series would be enough when the Fourier number is greater than 0.2 since the temperature change after that certain time would be linear (Becker and Fricke, 2004; Bimbenet et al., 2002; Caro-Corrales et al., 2002; Dincer, 1996; Erdogan, 2005). As long as the thermal diffusivity is constant, this first term approach may be easily used to determine the temperature change with Eq. (1) and with the known heat transfer coefficient value:

$k = \varphi^2 \cdot \alpha / l^2$ at any given position in the infinite slab where φ is the first root of the following equation:

$$\cot \varphi = \frac{\varphi}{Bi} \quad (3)$$

At the half thickness of the infinite slab,

$$j = \frac{2 \sin \varphi}{\varphi + \sin \varphi \cos \varphi} \quad (4a)$$

At the surface of the infinite slab,

$$j = \frac{2 \sin \varphi \cos \varphi}{\varphi + \sin \varphi \cos \varphi} \quad (4b)$$

With respect to the cooling/heating of the product during the initial ‘lag’ period ($Fo < 0.2$), we assumed a straight linear link between T_0 and temperature at time corresponding to $Fo = 0.2$.

2.2. Bacterial growth modelling

As a primary model, a simple exponential growth without lag time was assumed:

$$N = N_0 e^{\mu t} \quad (5)$$

Where N is the cell number at time t , N_0 is the initial cell number and μ the specific bacterial growth rate at time t .

The gamma function corresponds to a comparison between the growth rate of microbial cells growing at given environmental conditions and the optimum growth rate that would be measured at optimal conditions (Zwietering et al., 1992):

$$\Gamma = \frac{\mu}{\mu_{opt}} \quad (6)$$

In the framework of standard calculations aiming to compare processes to each others, a simplified gamma function depending only on temperature can be derived from the “square root” model of Ratkowsky et al. (1982) modified by Zwietering et al. (1992)

$$\gamma(T) = \left(\frac{T - T_{min}}{T_{opt} - T_{min}} \right)^2 \quad (7)$$

Where T_{min} is the temperature below which no microbial growth occurs and T_{opt} is the temperature at which the microbial growth is optimal.

If a process has to be intrinsically assessed regardless of the characteristics of the foodstuff, a partial proliferation value may be involved. If the local temperature at which the bacteria are growing is the single considered factor, Mafart (2005) defined a “thermal proliferation value” as:

$$f' = \int_0^t \gamma(T) dt \quad (8)$$

This value has the dimension of a time and corresponds to a time-temperature cycle that would yield the same proliferation ratio than a growth of f' units of time at the optimal and constant temperature (Mafart, 2005).

The original differential form of equation (6) is:

$$\frac{1}{N} \frac{d(N)}{dt} = \mu(t) = \mu_{opt} \gamma[T(t)] \quad (9)$$

the solution of which yields:

$$\frac{N}{N_0} = \exp \left[\mu_{opt} \int_0^t \left(\frac{T - T_{min}}{T_{opt} - T_{min}} \right)^2 dt \right] \quad (10)$$

This model can be easily combined with heat transfer models permitting the obtainment of an analytic solution yielding the overall model. Note that, even for complex foodstuff shapes, an analytic solution of the model is possible, provided that thermal parameters of equation (1) (j and k) can be empirically determined from a temperature registration and a linear regression of reduced temperature.

The concept of thermal proliferation value may be usefully completed by that of equivalent temperature, which corresponds to the constant temperature that would yield the same proliferation during the duration of a thermal cycle. A cooling/heating process can then be

characterised and be compared with others by its duration and its equivalent temperature (Mafart, 2005).

$$\gamma(T_{eq})t = f' \quad (11)$$

where time is expressed in hours. The combination of this last equation with Eq. (7) yields:

$$T_{eq} = T_{\min} + (T_{opt} - T_{\min}) \sqrt{\frac{f'}{t}} \quad (12)$$

2.3. Overall model

The overall model developed in the present study aims to consider the convective heat transfer coefficient and the temperature of the ambient medium when predicting bacterial growth under dynamic conditions of temperature.

Combining Eqs. (1) and (7) the obtained time-dependent $\gamma(T)$ function is employed in Eq. (8) in order to express, by integration, f' as a function of t :

$$f'(T) = \frac{k(T_{\infty} - T_{\min})^2 t + 2j(T_{\infty} - T_{\min})(T_0 - T_{\infty})(1 - e^{-kt}) + \frac{j^2}{2}(T_0 - T_{\infty})^2(1 - e^{-2kt})}{k(T_{opt} - T_{\min})^2} \quad (13)$$

The substitution of f' in Eq. (13) by its above-cited expression enables the calculation of the equivalent temperature as follows:

$$T_{eq} = T_{\min} + \sqrt{\frac{k(T_{\infty} - T_{\min})^2 t + 2j(T_{\infty} - T_{\min})(T_0 - T_{\infty})(1 - e^{-kt}) + \frac{j^2}{2}(T_0 - T_{\infty})^2(1 - e^{-2kt})}{kt}} \quad (14)$$

The implementation of the Eq. (10) to T_{eq} of the thermal process yields:

$$\frac{N}{N_0} = \exp \left[\mu_{opt} \left(\frac{T_{eq} - T_{\min}}{T_{opt} - T_{\min}} \right)^2 t \right] \quad (15)$$

The overall mathematical model corresponds to the association of these two last equations.

The determination of the j value at the centre (Eq. (4a)) or at the surface (Eq. (4b)) of an infinite slab allows the calculation of the corresponding T_{eq} values. The parameter k is

determined from Eq. (3) at any given position in the product and with Bi which includes the convective heat transfer coefficient h that will be changed in the experimental validation of the overall model.

3. Materials and methods

3.1. Micro-organism and inoculum preparation

E. coli SOR 201 (isolated from cheese), provided by SOREDAB Laboratory (France), was stored at -80 °C in nutrient broth supplemented with 50% glycerol. The inoculum was prepared by subculturing the bacterial strain in 100 mL of nutrient broth (tryptone 10 g/L, meat extract 5 g/L and sodium chloride 5 g/L. pH 7.2±0.2) at 37 °C on a rotary shaker (100 rpm), subsequently for 8 h and 16 h.

3.2. Experimental setup for the model validation at constant air temperature and changing convective heat transfer coefficient

3.2.1. Growth measurement

Growth curves were determined by the measurement of absorbance changes with a spectrophotometer (Milton Roy, Spectronic 301) at 600 nm wavelength. Absorbance was measured with sterile nutrient broth as a blank. Samples were filled in glass “growth flasks” specially designed for the measurement of the absorbance of the content without sampling. A calibration experiment was done to determine the correlation between viable counts and absorbance data in nutrient broth permitting the estimation of the bacterial concentrations from absorbance values. Samples were incubated at 30 °C in a shaking water bath and bacteria were grown until stationary phase. The optical density was periodically measured and one mL was simultaneously removed from the solution to be analyzed by the plate count method. The experimental dataset was fitted with the exponential model proposed by Juarez Tomas et al. (2002) to fit the calibration equation which can be written as follows:

$$\ln N = a(OD)^b \quad (16)$$

Where N is the bacterial concentration, OD is the corresponding optical density (600 nm) measured at time t and a and b are empirical parameters.

Fig. 1 depicts the experimental data and the calibration curve relating OD to viable counts. Estimates of parameters a and b were respectively assessed to 22.8 [22.6 .. 22.9] and 0.090 [0.087 .. 0.093] ($R^2 = 0.999$ and $MSE = 0.009$).

Francois et al. (2005) demonstrated that a temperature of 4 °C had no significant statistical effect on the linear calibration curve compared to optimal conditions (T 30 °C, pH 7,4 and a_w 0.995) in BHI medium. Consequently, we didn't perform the calibration experiment at other temperatures than 30 °C (the initial product temperature at all the experiments).

3.2.2. Simulation design

Five combinations of thickness of an infinite slab, convective heat transfer coefficient and chilling temperature were input (Fig. 2) for the calculation of thermal parameters j and k . A simulated growth curve related to each combination was then calculated from Eqs. (14) and (15). An h value of 8 W/(m².K) corresponds to the absence of fan (particularly in unventilated zones or in equipment inside which heat is transferred by natural convection) while an h value of 60 W/(m².K) corresponds to a strong air fan (in the case of forced convection). Moreover, according to Kondjoyan (2006), average heat transfer coefficient values (W/(m².K)) calculated under different air velocity (0.2 – 5.0 m s⁻¹) and free-stream turbulence intensity conditions (5 – 40 %) ranged from 1.3 to 42.0 for a circular cylinder and from 2.3 to 60.0 for meat products (Beef carcass, pork hindquarter and lamb carcass (loin)). Furthermore, Ben Amara et al. (2004) studied the effect of various factors (air velocity, position, air-product temperature difference) on the transfers during cooling with a low air velocity (< 0.2 m/s), of an in-line stack of spheres and measured h values ranging from 8 to 19 W/(m².K) for air velocity varying from 0.03 to 0.19 m s⁻¹.

3.2.3. Conditions of growth for the validation of the model

Corresponding to each combination of slab thickness and convective heat transfer coefficient, cooling profiles and bacterial growth were simulated at the centre and at the surface of an infinite slab shaped product. The product thermal diffusivity and thermal conductivity values input in the calculations were assumed to be equal to those of water determined at 25 °C, i.e. $1.43 \cdot 10^{-7} \text{ m}^2/\text{s}$ and $0.6 \text{ W}/(\text{m} \cdot \text{K})$ respectively.

Furthermore, input μ_{opt} , T_{min} and T_{opt} values of *E. coli* SOR 201 were respectively equal to 2.66 h^{-1} , 3.28 °C and 42.03 °C in nutrient broth. These values were estimated from forty six growth kinetics conducted at 11 constant temperatures ranging from 10 °C to 46 °C . Experimental datasets were fitted and growth curve parameters (maximum growth rate (μ_{max}), lag time, initial and maximum population densities) were estimated from the primary growth model of Baranyi and Roberts (1994). The obtained μ_{max} values were fitted with the secondary cardinal model (Rosso et al., 1995) in order to estimate the optimal growth rate and the cardinal temperatures of *E. coli* SOR 201 (see Fig. A2 in the appendix).

In order to validate the overall mathematical model developed in the present work, experiments were conducted under a changing temperature program which corresponds to the simulated cooling profiles of the surface or the centre of the product. All the prepared material was pre-chilled/heated to the initial temperature (30 °C). Subculture was diluted to provide an inoculation level ranging from 10^6 to 10^7 CFU/mL at the starting of the test. Samples were filled in glass “growth flasks” allowing the measurement of the absorbance of the content, during the experiment, without sampling. Their shaking was guaranteed by a magnetic shaking table. Samples were instantly incubated and periodically removed so as to measure optical densities (at 600 nm) in the course of the experiment. Experiments were carried out in triplicate. The chilling was monitored with a refrigerated and heating circulator (FP40-HE, Julabo Labortechnik GmbH, Germany) allowing a temperature stability of $\pm 0.01 \text{ °C}$.

3.3. Experimental setup for the model validation at changing air temperature and constant convective heat transfer coefficient

For a further validation of the model, more complicated temperature scenarios were tested assuming alternated cooling and heating stages. Moreover, an inoculation level ranging from 10^3 to 10^4 CFU/mL was used in order to consider more realistic bacterial concentrations encountered in food industry processes.

Three different ambient air temperature scenarios, drawn from real refrigerated food processes, were tested (cf. Table 2).

Corresponding to each air temperature scenario, temperature profiles and bacterial growth were simulated at the centre and at the surface of an infinite slab shaped product. At all the tested temperature scenarios, the initial product temperature, the product thickness and the convective heat transfer coefficient were respectively equal to 15 °C, 0.12 m and 8 W/(m².K). Input μ_{opt} , T_{min} and T_{opt} values of *E. coli* SOR 201 are mentioned above. Typical beef meat thermal diffusivity and thermal conductivity values, respectively equal to $1.25 \cdot 10^{-7}$ m²/s and 0.42 W/(m.K), were input in the calculations.

Experiments were conducted under thermal programs which corresponded to the simulated temperature profiles of the surface or the centre of the product. Subculture was diluted, samples were filled in glass “growth flasks”, instantly incubated and periodically removed so as to perform the viable count measurement in the course of the experiment. Experiments were carried out in duplicate. The thermal program was monitored with the refrigerated and heating circulator (FP40-HE, Julabo Labortechnik GmbH, Germany). At each sampling time, 1-mL aliquots were aseptically removed from each “growth flask”, serially diluted in tryptone salt broth and plated on nutrient agar (15 g/L) with a double layer. Petri dishes were incubated at 37 °C for 24 h and colonies were counted.

3.4. Validation and assessment of the quality of the overall model

Model accuracy was assessed by the estimation of confidence bands of predictions by using the bootstrap percentile method (Efron and Tibshirani, 1993). Forty six growth kinetics were performed in nutrient broth at 11 constant temperatures ranging from 10 °C to 46 °C (data not shown). Bootstrap of each kinetic was made in order to take the experimental errors of kinetics into account. The appropriate residuals of each kinetic were drawn with replacement. Twenty five thousands bootstrap set of primary parameters were obtained. Each set of bootstrapped μ_{max} values were used to fit the secondary model. Then bootstrapped values of parameters T_{min} , T_{opt} and μ_{opt} were used to predict the bacterial growth with the overall model. Secondary observed residuals were drawn with replacement and added to the μ predicted value. Primary residuals were added to the predicted kinetics to consider the experimental error of cell number estimation. Twenty five thousands bootstrapped growth kinetics were obtained for each validation experiment and sorted in ascending order at each calculation time. The quartiles 2.5% and 97.5% of the sorted bootstrapped kinetics were taken to give the inferior and superior limits. These points were linked to give an approximation of the 95 percent confidence bands of the predicted growth kinetics. To validate the assumptions made and the model, less than 5% of the points must fall outside the confidence bands.

With regard to the assessment of the quality of the overall model predictions various statistical criteria were calculated at all the tested conditions of validation experiments. Correlation coefficients (R) between observations and predictions were calculated using the ‘corrcoef’ function of MATLAB 6.5. The correlation coefficient is related to the covariance cov by:

$$R(i, j) = \frac{cov(i, j)}{\sqrt{cov(i, i)cov(j, j)}} \quad (17)$$

where i is the observations index and j is the variables index.

Bias factor B_f (Eq. (18)) and Accuracy factor A_f (Eq. (19)) were calculated as proposed by Jeyamkondan et al. (2001). These factors were initially introduced by Ross (1996) but here, the predicted values are normalized.

$$B_f = 10^{\sum \log(P/O)/n} \quad (18)$$

$$A_f = 10^{\sum |\log(P/O)|/n} \quad (19)$$

where O and P are observed and predicted microbial populations in \log_{10} CFU/mL and n is the number of observations. The bias factor indicates the relative average deviation of predicted and observed bacterial growth. However it has to be kept in mind that this deviation does not directly concern the size of the population, but its logarithmic transformation which reduces the effect of outliers.

A bias factor of 1 indicates perfect agreement between observed and predicted values. However, $B_f > 1$ or < 1 indicates that the model predicts N upper than or lower than observed values. For example, $B_f = 1.1$ means that predictions are on average upper than observed values by 10%. The accuracy factor gives indication of the spread of the results about the predicted value. An accuracy factor of 1 represents perfect agreement between observed and predicted values. This parameter quantifies the difference between observed and predicted values. For example, $A_f = 1.25$ indicates that the average deviation of the predicted values from the observed values is 25%. It has to be kept in mind that this deviation does not directly concern the size of the population, but its logarithmic transformation.

4. Results

4.1. Model validation at constant air temperature and changing convective heat transfer coefficient

4.1.1. Growth simulation

Thermal programs tested at the validation stage were utilized at five different combinations of product thickness (E), convective heat transfer coefficient (h) and refrigeration temperature

(T_{∞}) (Fig. 2).

The obtained cooling profiles and growth predictions are presented in Fig. 3. As a rule, bacterial growth kinetics were faster at the product centre than at its surface. In cases of lowest thickness, simulated computing profiles (1c and 2c) were practically identical leading to the same bacterial growth predictions (1g and 2g) at the centre and at the surface of the product. In fact, in these two experiments the product thickness was sufficiently low to prevent a clear observation of an internal temperature gradient and the internal heat resistance may have been neglected. In contrast, the difference between simulated theoretical temperature kinetics at the centre and the surface of the product were more marked in the cases of the highest thickness leading to an important thermal gradient within the product (3c and 4c). For that matter, the most important differences between internal and surface growth kinetics were obtained in these two cases (3g and 4g), particularly in the case of low heat transfer coefficient.

On the other hand, additional simulated growth curves at constant temperatures equal to T_{∞} were presented in Fig. 3. The aim of these further experiments was to compare the bacterial growth that really occurs when temperature dynamic changes at the centre and at the surface of the cooled product are considered, with the growth that would occur if external and internal resistances were neglected.

4.1.2. Validation results

Each validation experiment regarding each (T_{∞} , h , E) combination (Fig. 2) was conducted under two different refrigeration programs which corresponded to the simulated cooling of the surface and the centre of the infinite slab-shaped product yielding a total of eight validation tests. These tests lasted 24 hours with an initial temperature T_0 of 30 °C. In order to validate the overall mathematical model, Fig. 4 depicts predicted and observed *E. coli* SOR 201 growth during the simulated cooling at the centre or the surface of the product for the five

cases presented in Fig. 2. A fair agreement between predicted and observed growth can be noted, and the observed growth data of *E. coli* SOR 201 were found to be adequately predicted by the overall mathematical model. For each predicted growth kinetic, 95 percent confidence bands calculated with bootstrap method are also presented in Fig. 4. All the experimental data fell inside the confidence bands showing that the overall model was successfully validated at the tested conditions.

On the other hand, the quality of the overall model prediction was assessed by the calculation of correlation coefficient, B_f and A_f (see Table 3). The correlation coefficients were higher than 0.975 showing that the bacterial growth was satisfactorily predicted by the overall model. At all the instances, bias factors ranged from 0.98 to 1.00 indicating that ~~on average, the observed growth was at the most 2% higher than the predicted growth and that~~ the overall predictions agreed well with observed data with a slight under-prediction tendency by the model. ~~In all the tested conditions, the percentage of predicted values which were different (either above or below) than the observed values was at the most equal to 5% as can be noted from A_f values ranging from 1.01 to 1.05.~~

Agreement between model predictions and experimental validation results was also assessed by plotting predicted bacterial growth versus observed bacterial growth (Fig. 5). A perfect agreement between predicted and measured growth was observed for 30.80% of experimental data. A percentage of 25.36% of the observed–predicted values’ pairs were laying under the line of equivalence while 43.84% were laying above the line of equivalence.

4.2. Model validation at changing air temperature and constant convective heat transfer coefficient

4.2.1. Growth simulation

Fig. 6 illustrates the simulated thermal profiles and bacterial growth kinetics according to the conditions presented in Table 2 and §3.3. Thermal and bacterial growth simulation results

showed important differences of temperature profiles and growth between the product centre, the product surface and the ambient air. During heating, the highest bacterial growth was observed when simulations were carried out at air temperature, followed by the product's surface and then by the product's centre. Conversely, an opposite trend was observed during cooling. From a safety point of view, neglecting heat transfer phenomena that occur inside the product and between the ambient air and the product is more dangerous at cooling stages than at heating stages. Nevertheless this hazard depends on the temperature and duration history of the cooling/heating stages. Consequently it's very important to take into account the actual temperature of the product surface or centre rather than the ambient air temperature for a reliable bacterial growth prediction.

4.2.2. Validation results

Validation results regarding the three tested ambient scenarios are presented in figures 7 and 8. The observed growth data of *E. coli* SOR 201 were found to be adequately predicted by the overall mathematical model. On the other hand, less than 5% of the experimental data fell outside the 95 percent confidence bands showing that the overall model was successfully validated at the tested conditions. Table 4 presents the statistical criteria related to the data of validation at changing air temperature and shows correlation coefficients higher than 0.944 at all the tested conditions. Bias factors obtained at all the assays were higher than 1 showing a slight over-prediction tendency by the model. A_f values (lower than 1.13 at all the instances) indicate that the overall predictions agreed well with observed data. Fig. 8 shows predicted bacterial growth versus observed bacterial growth and confirms that the overall model was successfully validated, with a slight over-prediction tendency, for the tested dynamic refrigeration cycles.

5. Discussion

455 Traditionally, when simulating a bacterial growth during a product cooling or heating,
456 predictive microbiology took only the ambient air temperature into account, ignoring delays
457 and temperature gradients due to external and internal thermal resistances linked to the effects
458 of the medium thickness and of the convective heat transfer coefficient on the rate of heat
459 transfer. All the studies cited in Table 1 have evaluated the prediction of bacterial growth
460 under dynamic temperature conditions taking into account only the temperature of the
461 cooling/heating medium. Assuming that the bacterial growth directly occurs at the
462 temperature of air is not valid. In fact, the local temperature at any given position in the
463 product depends upon both T_{∞} and h . In the present study, predictive microbiology was
464 combined with heat transfer phenomena in order to develop an overall mathematical model
465 describing the effect of the ambient temperature and the convective heat transfer coefficient
466 on bacterial growth. The proposed method in this work is different than those in previous
467 studies which combined predictive microbiology and heat transfer (Alavi et al., 2001;
468 Amezcuita et al., 2005; Bellara et al., 2000; Corradini et al., 2006). An experimental method
469 was implemented in order to validate the model results. Thermal profiles were firstly
470 simulated at the centre and at the surface of the infinite slab shaped product. Then,
471 experiments were conducted under a changing temperature program corresponding to the
472 simulated temperature kinetics. The validation of the overall model was performed by the
473 comparison of the measured bacterial growths with model predictions at constant ambient air
474 temperature and changing convective heat transfer coefficient and product thickness (five
475 different combinations of product thickness, convective heat transfer coefficient and cooling
476 air temperature were tested), then at changing ambient air temperature and fixed convective
477 heat transfer coefficient and product thickness (three different ambient air scenarios assuming
478 alternated cooling and heating stages, drawn from real refrigerated food processes, were
479 tested).

As expected, the results of the computer simulation related to single cooling stage experiments showed that the bacterial growth kinetics were faster at the product centre than at its surface. Moreover, the importance of the impact of the convective heat transfer coefficient and of the product thickness on the bacterial growth during the cooling of an infinite slab shaped product by pulsed air was pointed out. As an example, at the product half thickness, the level of bacterial growth accomplished after 5 hours of cooling with $h = 8 \text{ W}/(\text{m}^2.\text{K})$ (case 3) was the same after 16.5 hours with $h = 60 \text{ W}/(\text{m}^2.\text{K})$ (case 4). For these cases the product thickness was the same and the cooling air temperature was in case 3 4°C lower than in case 4. Similarly, at product half thickness, the cooling time needed to reach a same bacterial growth with low or high product thickness (1 cm in case 2 and 6 cm in case 4) was estimated to 17.5 hours and 8 hours, respectively, for the same convection level ($60 \text{ W}/(\text{m}^2.\text{K})$). The slowest simulated bacterial growth was observed with intermediate product thickness and convective heat transfer coefficient (case 5). Moreover, it obviously appears that the validity of the assumption of an instantaneously thermal equilibrium between the product and the cooling medium with regard to bacterial growth is depending on the level of convection. In fact, predicted growth kinetics at the surface of the product were close to those predicted at T_∞ for high heat transfer coefficients (h) equal to $60 \text{ W}/(\text{m}^2.\text{K})$, which corresponds to a strong air fan (Fig. 3: 2g and 4g). At this instance, neglecting the external heat resistance may be accepted particularly for low product thickness (1 cm) where there's no internal heat resistance too. Oppositely, for low heat transfer coefficients (h) equal to $8 \text{ W}/(\text{m}^2.\text{K})$, which corresponds to the absence of fan, (Fig. 3: 1g and 3g) important dissimilarities between predicted growth kinetics at the surface of the product and at T_∞ may be observed. Indeed, assuming no external heat transfer resistance is not valid especially for high product thickness of 6 cm (Fig. 3: 3g) where the bacterial growth that occurs when the product is cooled from T_0 to T_∞ was clearly higher than that at an immediately reached temperature T_∞ . In this case, a

difference of 1.35 log₁₀(CFU/mL) between the bacterial populations at the product surface and at T_{∞} was reached after 24 hours of growth. Besides, using the bootstrap percentile method for the estimation of confidence bands of predictions, the model was successfully validated at all the tested conditions.

Concerning the results related to alternated cooling and heating stage experiments, the model was successfully validated at more complicated ambient air scenarios and lower inoculation levels by plate count measurement method. These results showed that, in predictive microbiology, assuming an instantaneously thermal equilibrium between the product and the ambient medium is not valid and may have large consequences on risk assessment of refrigerated food processes (see Fig. 9).

To assess the quality of the overall model, predicted bacterial growth was compared to observed growth according to several statistical criteria related to the data of validation. Our results pointed out a good agreement between predicted and observed growth.

On the other hand, in the overall model, as a primary bacterial model, a simple exponential growth without lag time was assumed. In other words, it is supposed that the bacterial growth occurred without delay when the product temperature was continuously changing. Our assumption is in agreement with several previous studies. Although the fact that organisms need to adapt to the new temperature, so that they go through a lag phase caused by the stress of the temperature shift, was largely noticed in literature (Amezquita et al., 2005; Baranyi et al., 1995; Koutsoumanis, 2001; Zwietering et al., 1994), the lag phase duration was rarely considered in predictive models. In accordance with our work, no further delay occurring after temperature shifts, once a cell population is growing exponentially, was frequently assumed (Baranyi et al., 1995; Bovill et al., 2000; Koutsoumanis et al., 2006). Although, Swinnen et al. (2005) demonstrated that temperature shifts crossing a lag/no lag transition zone (positioned more or less between 22.78 and 23.86 °C for *E. coli* K12 MG1655) will cause an intermediate

lag phase, we consider that neglecting contingent intermediate lag phase by our model may be a valid approach. In fact, simulated thermal profiles at product surface or centre due to heat transfer phenomena (see Fig. 3 and Fig. 6) progressively changed with time and cannot be regarded as instantaneous temperature shifts with given amplitude which may generate intermediate lag phases.

Paradoxically, the complexity of foods' shapes and the lack of knowledge about their physical properties dictate the utilization of simple model. We took as an example the case of infinite slab, but the model can be generalised to complex shapes. A classical and relevant approach is of course, the implementation of numerical modelling. Another approach is related to the well-known Ball method (Ball, 1923) with its two empirical parameters, for heat treatment processes calculations. Because foodstuffs shapes are complex and because their thermal properties are often unknown, it can be relevant to implement a simple model including only two parameters (j and k of Eq. (1)) which can be easily empirically estimated from a simple temperature registration and a simple linear regression of the reduced temperature (which is linearised from a logarithmic transformation). Note that errors which can be generated by "simplistic" heat transfer models are minor compared to errors which are linked to the "biological background". Moreover, the overall model can be used for any bacterial strain having known growth parameters T_{min} , T_{opt} and μ_{opt} . Accordingly, the proposed model can be used for designing safe cooling or heating processes and may be considered as a very useful tool for risk assessment regarding food safety and process optimisation.

6. Appendix

Equation of the the infinite series given by Carslaw and Jaeger (1986):

$$\frac{T_{\infty} - T}{T_{\infty} - T_0} = \sum_{n=1}^{\infty} \frac{2 \sin \varphi_n}{\varphi_n + \sin \varphi_n \cos \varphi_n} \cos\left(\varphi_n \frac{x}{x_{\max}}\right) \exp(-\varphi_n^2 Fo) \quad (20)$$

with x_{\max} is half-thickness for an infinite slab and φ_n are the roots of the equation $\cot \varphi = \frac{\varphi}{Bi}$.

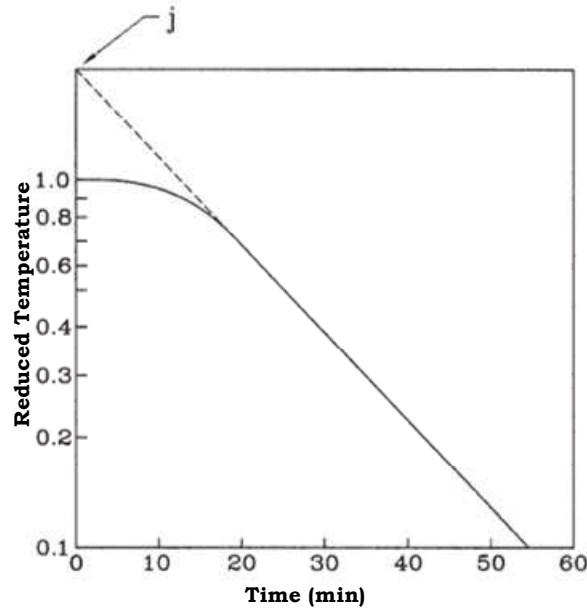


Fig. A1. Typical cooling curve (Becker and Fricke, 2004)

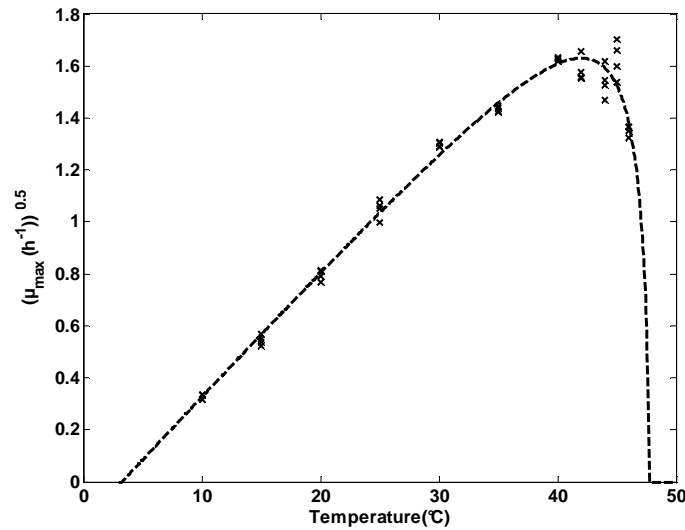


Fig. A2. Fit of the cardinal model on μ_{\max} values measured in nutrient broth (x). The dashed line denotes the fitted model on the experimental data.

References

- Alavi, S.H., Puri, V.M., Mohtar, R.H. 2001. A model for predicting the growth of *Listeria monocytogenes* in packaged whole milk. *Journal of Food Process Engineering* 24, 231–251.
- Amezquita, A., Weller, C.L., Wang, L., Thippareddi, H., Burson, D.E. 2005. Development of an integrated model for heat transfer and dynamic growth of *Clostridium perfringens* during the cooling of cooked boneless ham. *International Journal of Food Microbiology* 101, 123-144.
- Armitage, N.H. 1997. Use of predictive microbiology in meat hygiene regulatory activity. *International Journal of Food Microbiology* 36, 103-109.
- Ball, C. 1923. Thermal process times for canned foods. Bulletin 7-1, 37 (National Research Council, Washington, DC).
- Baranyi, J., Roberts, T.A. 1994. A dynamic approach to predicting bacterial growth in food. *International Journal of Food Microbiology* 23, 277-294.
- Baranyi, J., Robinson, T.P., Kaloti, A., Mackey, B.M. 1995. Predicting growth of *Brochothrix thermosphacta* at changing temperature. *International Journal of Food Microbiology* 27, 61-75.
- Becker, B.R., Fricke, B.A. 2004. Heat transfer coefficients for forced-air cooling and freezing of selected foods. *International Journal of Refrigeration* 27, 540-551.
- Bellara, S.R., McFarlane, C.M., Thomas, C.R., Fryer, P.J. 2000. The growth of *Escherichia coli* in a food simulant during conduction cooling: combining engineering and microbiological modelling. *Chemical Engineering Science* 55, 6085-6095.

583 Ben Amara, S., Laguerre, O., Flick, D. 2004. Experimental study of convective heat
 584 transfer during cooling with low air velocity in a stack of objects. International Journal of
 585 Thermal Sciences 43, 1213-1221.

586 Bimbenet, J.J., Duquenoy, A., Trystram, G. 2002. Génie des procédés alimentaires. Des
 587 bases aux applications. Dunod ed., Paris, France.

588 Bovill, R., Bew, J., Cook, N., D'Agostino, M., Wilkinson, N., Baranyi, J. 2000.
 589 Predictions of growth for *Listeria monocytogenes* and *Salmonella* during fluctuating
 590 temperature. International Journal of Food Microbiology 59, 157–165.

591 Bovill, R.A., Bew, J., Baranyi, J. 2001. Measurements and predictions of growth for
 592 *Listeria monocytogenes* and *Salmonella* during fluctuating temperature II. Rapidly changing
 593 temperatures. International Journal of Food Microbiology 67, 131–137.

594 Caro-Corrales, J., Cronin, K., Abodayeh, K., Gutiérrez-López, G., Ordorica-Falomir, C.
 595 2002. Analysis of random variability in biscuit cooling. Journal of Food Engineering 54, 147-
 596 156.

597 Carslaw, H.S., Jaeger, J.C. 1986. Conduction of Heat in Solids. 2nd ed. Oxford
 598 University Press.

599 Corradini, M.G., Amézquita, A., Normand, M.D., Peleg, M. 2006. Modeling and
 600 predicting non-isothermal microbial growth using general purpose software. International
 601 Journal of Food Microbiology 106, 223–228.

602 Dalgaard, P. 1995. Modelling of microbial activity and prediction of shelf life for
 603 packed fresh fish. International Journal of Food Microbiology 26, 305-317.

604 de Jong, A.E.I., Beumer, R.R., Zwietering, M.H. 2005. Modeling growth of *Clostridium*
 605 *perfringens* in pea soup during cooling. Risk Analysis: An International Journal 25, 61-73.

606 Dincer, I. 1996. An exact solution on the estimation of heat-transfer rates during deep-
 607 freezing of slab products. Journal of Food Engineering 30, 417-423.

608 Efron, B., Tibshirani, R.J. 1993. Confidence intervals based on bootstrap percentiles. In:
 609 An introduction to the Bootstrap. Chapman and Hall, New York, pp. 168-177.

610 Erdogdu, F. 2005. Mathematical approaches for use of analytical solutions in
 611 experimental determination of heat and mass transfer parameters. Journal of Food
 612 Engineering 68, 233-238.

613 Francois, K., Devlieghere, F., Standaert, A.R., Geeraerd, A.H., Cools, I., Van Impe,
 614 J.F., Debevere, J. 2005. Environmental factors influencing the relationship between optical
 615 density and cell count for *Listeria monocytogenes*. Journal of Applied Microbiology 99, 1503-
 616 1515.

617 Fujikawa, H., Kai, A., Morozumi, S. 2004. A new logistic model for *Escherichia coli*
 618 growth at constant and dynamic temperatures. Food Microbiology 21, 501–509.

619 Gibson, A.M., Bratchell, N., Roberts, T.A. 1987. The effect of sodium chloride and
 620 temperature on the rate and extent of growth of *Clostridium botulinum* type A in pasteurized
 621 pork slurry. Journal of Applied Bacteriology 62, 479-490.

622 Gill, C.O., Harrison, J.C.L. 1985. Evaluation of the hygienic efficiency of offal cooling
 623 procedures. Food Microbiology 2, 63-69.

624 Gumudavelli, V., Subbiah, J., Thippareddi, H., Velugoti, P.R., Froning, G. 2007.
 625 Dynamic predictive model for growth of *Salmonella Enteritidis* in egg yolk. Journal of Food
 626 Science 72, M254-M262.

627 Huang, L. 2003. Dynamic computer simulation of *Clostridium perfringens* growth in
 628 cooked ground beef. International Journal of Food Microbiology 87, 217–227.

629 Jeyamkondan, S., Jayas, D.S., Holley, R.A. 2001. Microbial growth modelling with
 630 artificial neural networks. International Journal of Food Microbiology 64, 343-354.

631 Juarez Tomas, M.S., Bru, E., Wiese, B., de Ruiz Holgado, A.A.P., Nader-Macias, M.E.
 632 2002. Influence of pH, temperature and culture media on the growth and bacteriocin

633 production by vaginal *Lactobacillus salivarius* CRL 1328. Journal of Applied Microbiology
634 93, 714-724.

635 Juneja, V.K., Marks, H., Thippareddi, H. 2008. Predictive model for growth of
636 *Clostridium perfringens* during cooling of cooked uncured beef. Food Microbiology 25, 42-
637 55.

638 Kondjoyan, A. 2006. A review on surface heat and mass transfer coefficients during air
639 chilling and storage of food products. International Journal of Refrigeration 29, 863-875.

640 Koseki, S., Isobe, S. 2005. Prediction of pathogen growth on iceberg lettuce under real
641 temperature history during distribution from farm to table. International Journal of Food
642 Microbiology 104, 239–248.

643 Koutsoumanis, K. 2001. Predictive modeling of the shelf life of fish under
644 nonisothermal conditions. Applied and Environmental Microbiology 67, 1821–1829.

645 Koutsoumanis, K., Stamatiou, A., Skandamis, P., Nychas, G.J.E. 2006. Development of
646 a microbial model for the combined effect of temperature and pH on spoilage of ground meat,
647 and validation of the model under dynamic temperature conditions. Applied and
648 Environmental Microbiology 72, 124-134.

649 Lebert, I., Lebert, A. 2006. Quantitative prediction of microbial behaviour during food
650 processing using an integrated modelling approach: a review. International Journal of
651 Refrigeration 29, 968-984.

652 Mafart, P. 1997. Génie industriel Alimentaire. Tome 1: Les procédés physiques de
653 conservation. Lavoisier Techniques & Documentations ed., Paris, France.

654 Mafart, P. 2005. Food engineering and predictive microbiology: on the necessity to
655 combine biological and physical kinetics. International Journal of Food Microbiology 100,
656 239-251.

657 McMeekin, T.A., Brown, J., Krist, K., Miles, D., Neumeyer, K., Nichols, D.S., Olley, J.,
658 Presser, K., Ratkowsky, D.A., Ross, T., Salter, M., Soontranon, S. 1997. Quantitative
659 Microbiology: A Basis for Food Safety. *Emerging Infectious Diseases* 3, 541-550.

660 McMeekin, T.A., Olley, J.N., Ross, T., Ratkowsky, D.A. 1993. *Predictive*
661 *Microbiology: theory and application* Research Studies Press, Taunton, Somerset, England.

662 Ratkowsky, D.A., Olley, J., McMeekin, T.A., Ball, A. 1982. Relationship between
663 temperature and growth rate of bacterial cultures. *Journal of Bacteriology* 149, 1-5.

664 Ross, T. 1996. Indices for performance evaluation of predictive models in food
665 microbiology. *Journal of Applied Bacteriology* 81, 501-508.

666 Rosso, L., Lobry, J.R., Bajard, S., Flandrois, J.P. 1995. Convenient model to describe
667 the combined effects of temperature and pH on microbial growth. *Applied and Environmental*
668 *Microbiology* Vol. 61, p. 610–616.

669 Swinnen, I.A.M., Bernaerts, K., Gysemans, K., Van Impe, J.F. 2005. Quantifying
670 microbial lag phenomena due to a sudden rise in temperature: a systematic macroscopic
671 study. *International Journal of Food Microbiology* 100, 85.

672 U.S.D.A. 1999. Performance standards for the production of certain meat and poultry
673 products. Final rule. *Federal Register* 64, 732-749.

674 Zwietering, M.H., De Koos, J.T., Hasenack, B.E., De Wit, J.C., Van't Riet, K. 1991.
675 Modeling of bacterial growth as a function of temperature. *Applied and Environmental*
676 *Microbiology* 57, 1094-1101.

677 Zwietering, M.H., De Wit, J.C., Cuppers, H.G.A.M., Van't Riet, K. 1994. Modeling of
678 bacterial growth with shifts in temperature. *Applied and Environmental Microbiology* 60,
679 204-213.

680 Zwietering, M.H., Hasting, A.P.M. 1997. Modelling the hygienic processing of foods -
681 Influence of individual process stages. *Food and Bioproducts Processing* 75, 168-173.

682 Zwietering, M.H., Wijtzes, T., de Wit, J.C., Van't Riet, K. 1992. A decision support
683 system for prediction of the microbial spoilage in foods. *Journal of Food Protection* 55, 973-
684 979.
685
686

Figure captions

Fig. 1.

Calibration curve between viable counts and absorbance data depicted with solid line. Experimental data measured at 30°C in nutrient broth are marked with (o).

Fig. 2.

Experimental design implemented for the validation of the overall model at different combinations (mentioned with numbers from 1 to 5) of product thickness (E), convective heat transfer coefficient (h) and refrigeration temperature (T_{∞}).

Fig. 3.

Cooling scenarios (from 1c to 5c) and bacterial growth curves (from 1g to 5g) obtained from simulation of the overall model at the five cases of the experimental design. Symbols in predicted cooling profiles: temperature of product centre (line —) and temperature of product surface (line — · —). Symbols in predicted growth curves: bacterial growth at product centre (line —), bacterial growth at product surface (line — · —) and bacterial growth that occurs at T_{∞} (line).

Fig. 4.

Comparison of predicted and observed *Escherichia coli* SOR 201 growth during cooling. **a**: case1 at the centre or the surface of the product. **b**: case2 at the centre or the surface of the product. **c**: case3 at the product centre. **d**: case3 at the product surface. **e**: case4 at the product centre. **f**: case4 at the product surface. **g**: case5 at the product centre. **h**: case5 at the product surface. Symbols in experimental data: o, □, Δ. Predicted growth curves estimated by the overall model are presented with (line —). 95 percent confidence bands obtained with bootstrap method are presented with (line — —).

Fig. 5.

Predicted bacterial growth from the overall model versus observed bacterial growth obtained with constant air temperature. Symbols: \square (case 1), \circ (case 2). Symbols related to product surface experiments: $*$ (case 3), Δ (case 4), \diamond (case 5). Symbols related to product centre experiments: \bullet (case 3), $+$ (case 4), \times (case 5). The line of equivalence between predicted and observed growth is marked with (line —).

Fig. 6.

Thermal profiles (from 1c to 3c) and bacterial growth curves (from 1g to 3g) obtained by simulation of the overall model at the three ambient air scenarios. Symbols in predicted cooling profiles: temperature of product centre (line —) and temperature of product surface (line — \cdot —). Symbols in predicted growth curves: bacterial growth at product centre (line —), bacterial growth at product surface (line — \cdot —) and bacterial growth that occurs at T_{∞} (line).

Fig. 7.

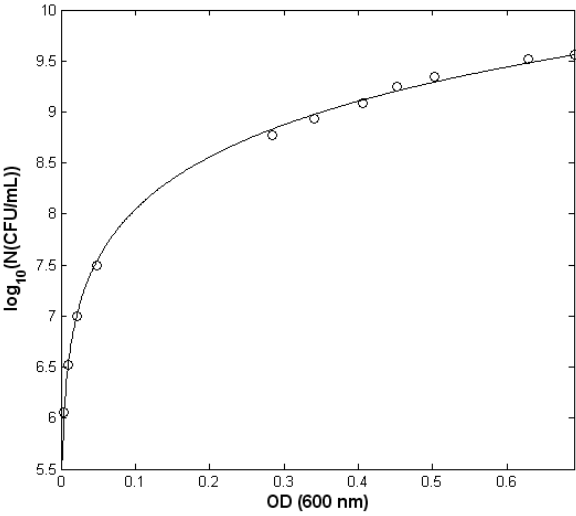
Comparison of predicted and observed *Escherichia coli* SOR 201 growth during thermal processing at changing air temperature. **a**, **c** and **e** depict the model validation results at the product centre according to cycle N°1, cycle N°2 and cycle N°3, respectively. **b**, **d** and **f** depict the model validation results at the product surface according to cycle N°1, cycle N°2 and cycle N°3, respectively. Symbols in experimental data: \circ , \square . Predicted growth curves estimated by the overall model are presented with (line —). 95 percent confidence bands obtained with bootstrap method are presented with (line — —).

Fig. 8.

Predicted bacterial growth from the overall model versus observed bacterial growth obtained with changing air temperature. Symbols related to product surface experiments: \square (Cycle N°1), $*$ (Cycle N°2), Δ (Cycle N°3). Symbols related to product centre experiments: \circ (Cycle N°1), \bullet (Cycle N°2), $+$ (Cycle N°3). The line of equivalence between predicted and observed growth is marked with (line —).

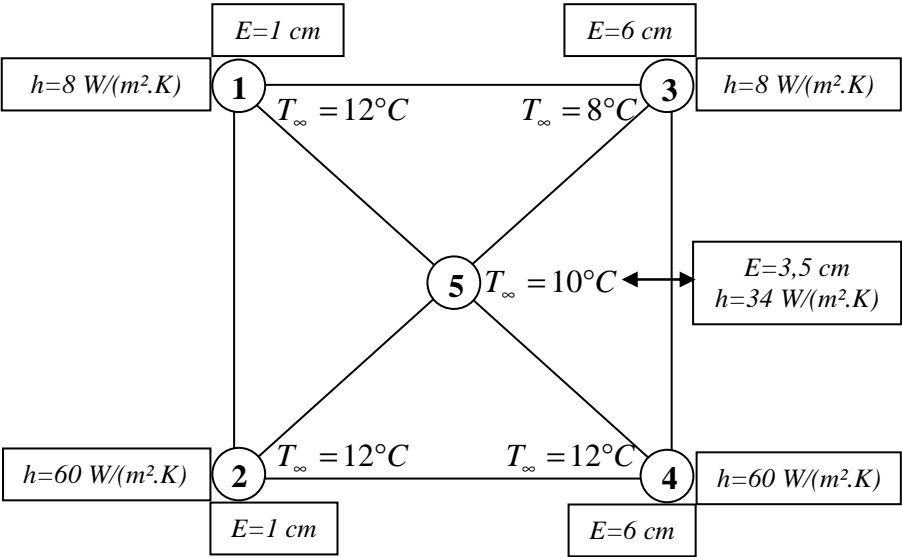
753 Fig. 9.
754 Comparison of the bacterial growth prediction at ambient temperature according to cycle N°1
755 with the model validation results at product's centre (*a*) and at product's surface (*b*). Symbols
756 in experimental data: o, □. Symbols in predicted growth curves: bacterial growth at product's
757 surface or centre (line —), bacterial growth that occurs at T_{∞} (line). 95 percent confidence
758 band of predictions at T_{∞} obtained with bootstrap method is presented with (line — —).

759
760



761
762
763 Fig. 1.

764



765

766

767

Fig. 2.

768

769

770

771

772

773

774

775

776

777

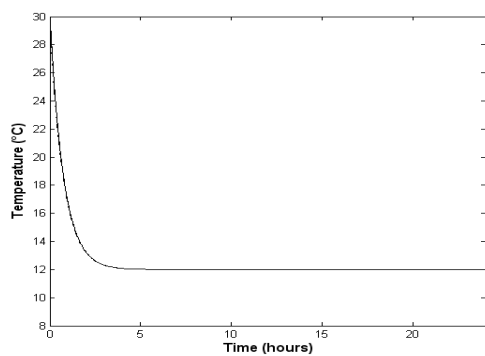
778

779

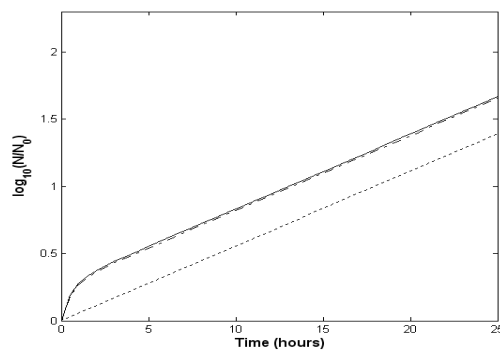
780

781

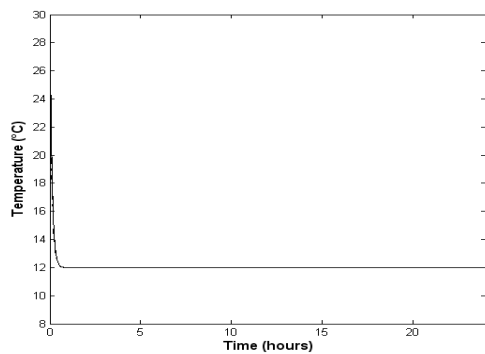
782



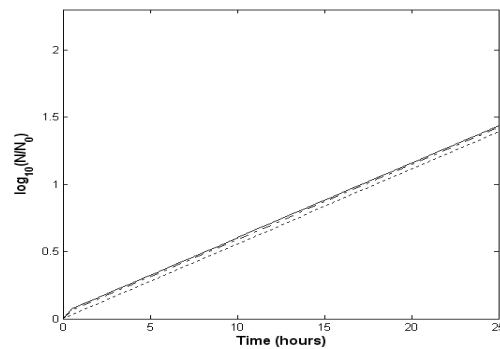
1c



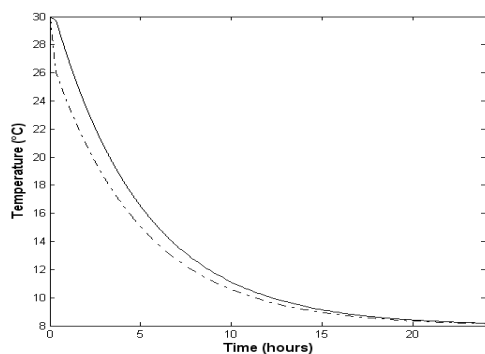
1g



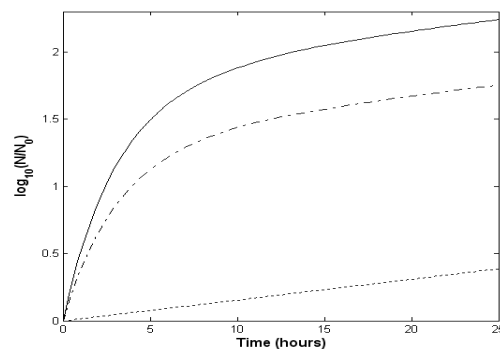
2c



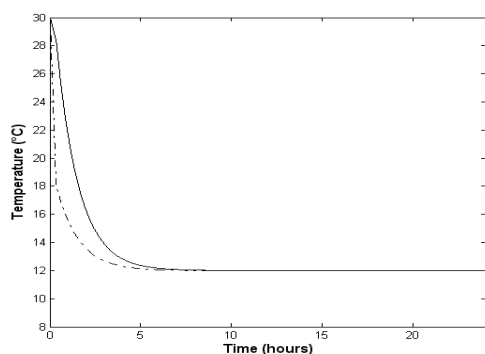
2g



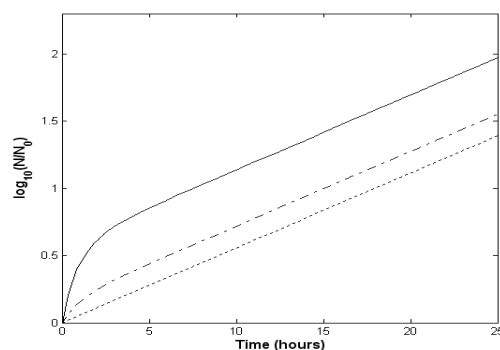
3c



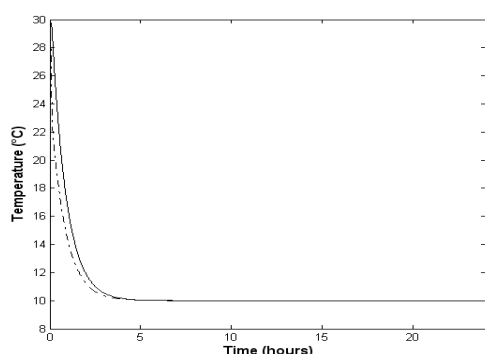
3g



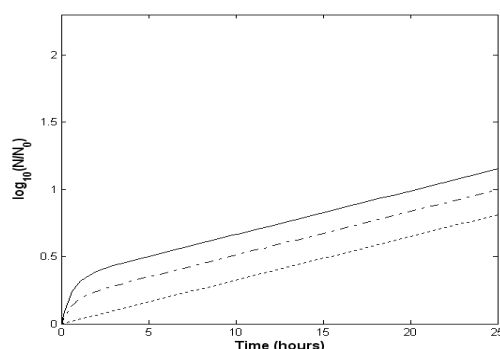
4c



4g



5c



5g

783 Fig. 3.

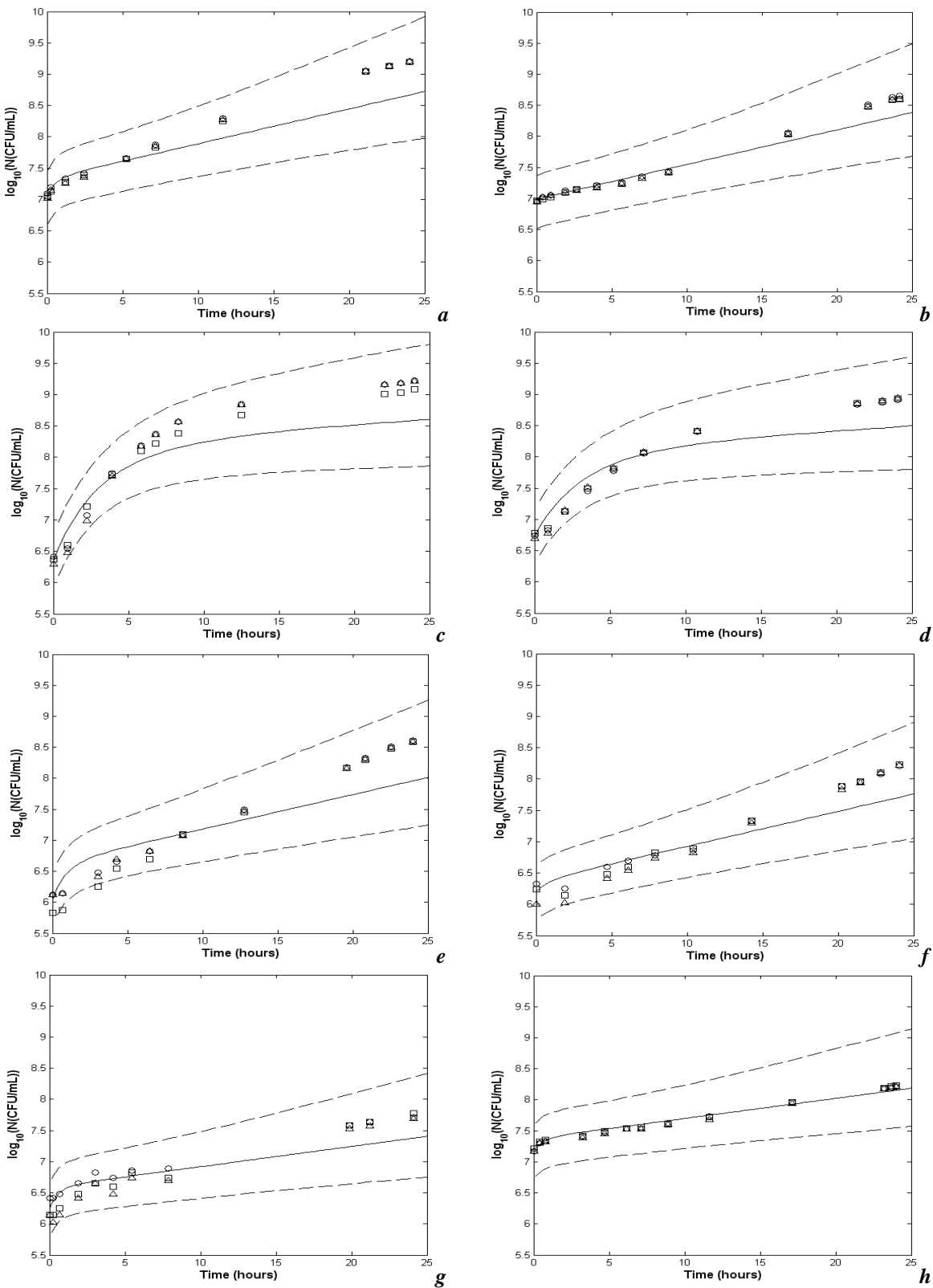


Fig. 4.

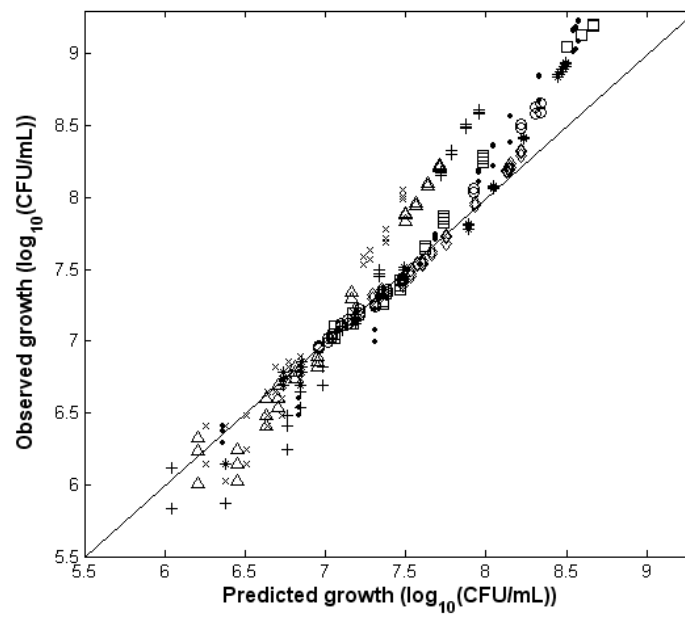
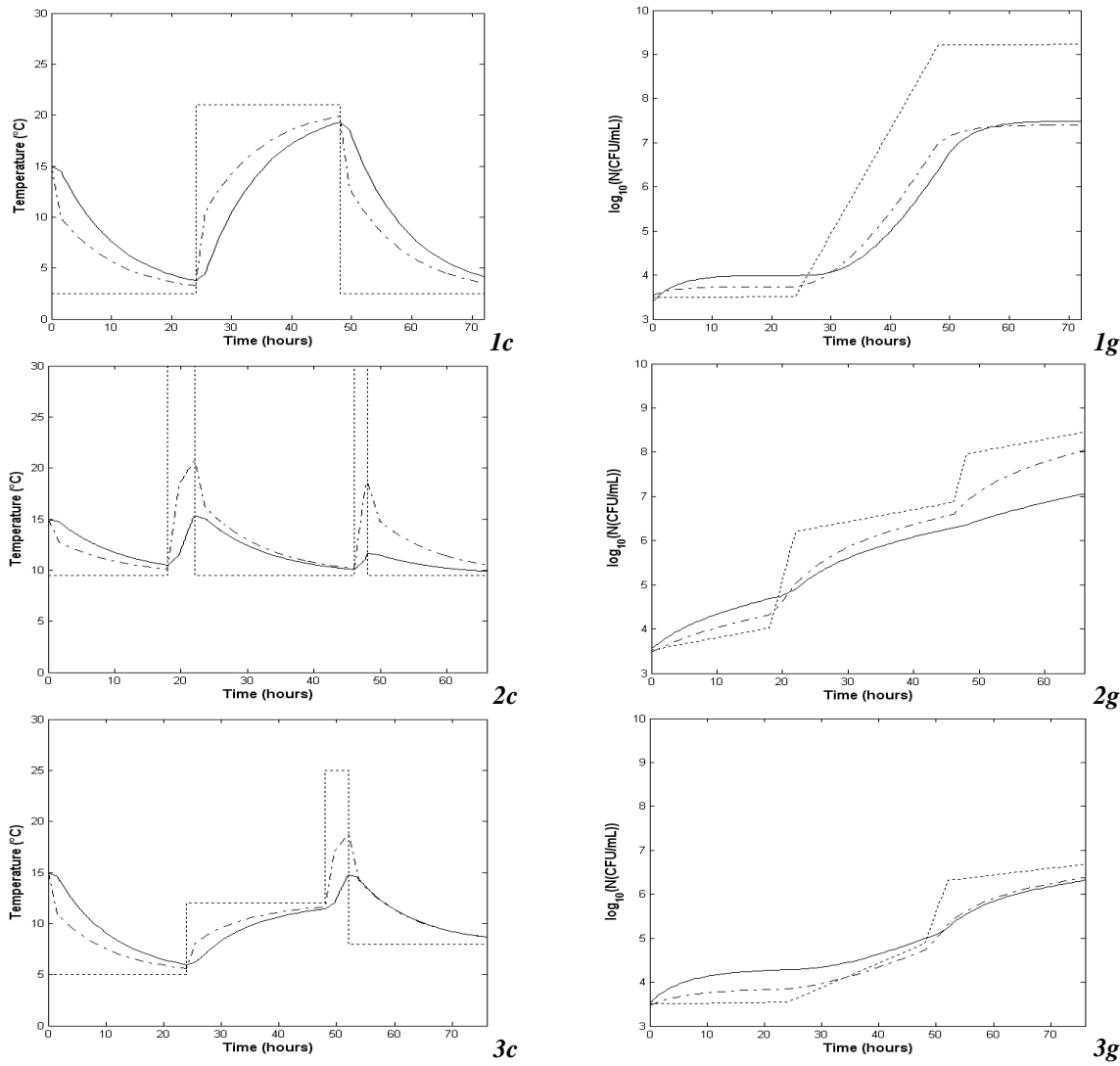
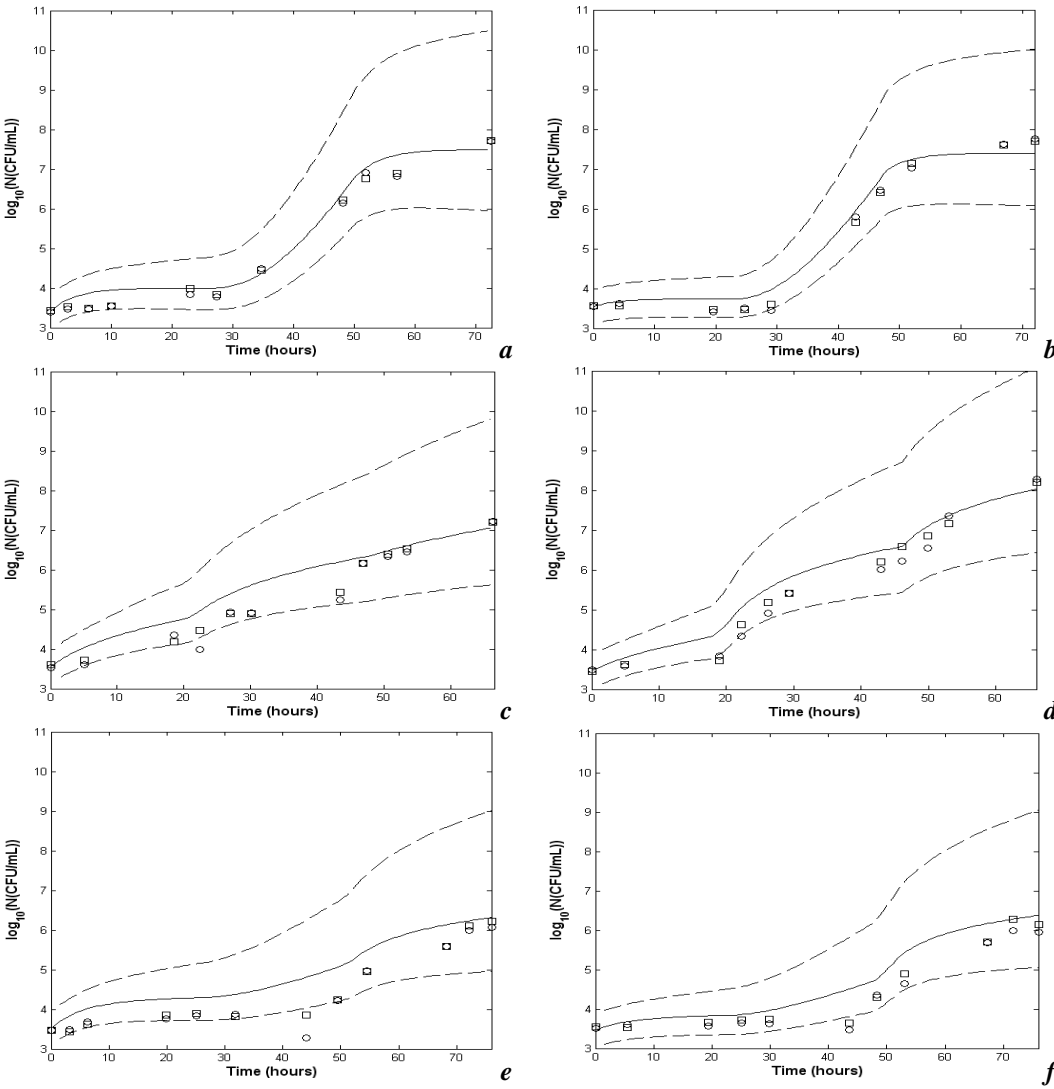


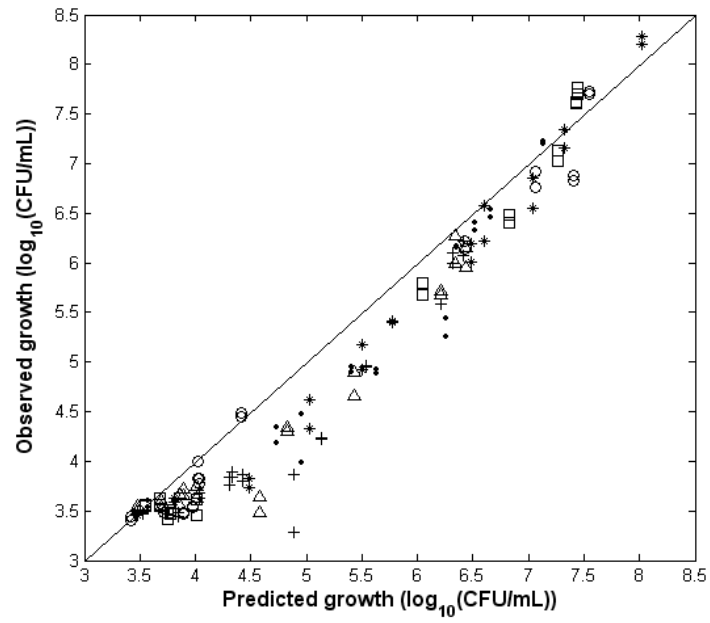
Fig. 5.



793 Fig. 6.



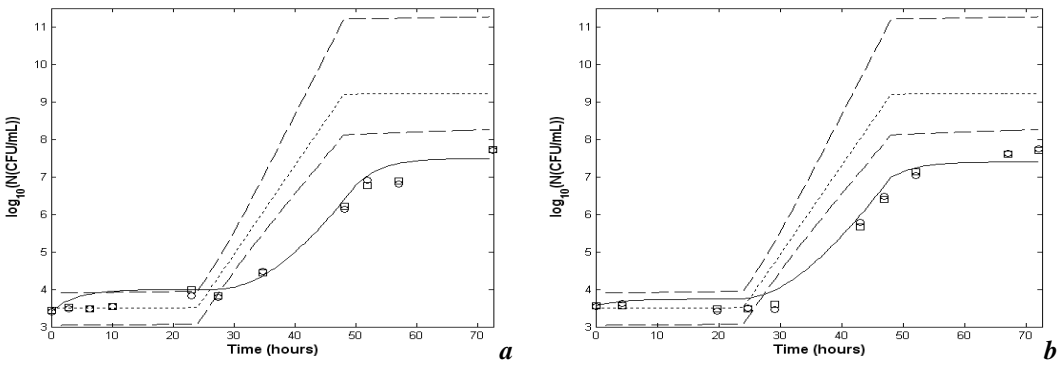
795 Fig. 7.



796

797 Fig. 8.

798



799

800

801 Fig. 9.

802

803 Table 1
 804 List of previous works dealing with models predicting the bacterial growth under dynamic
 805 temperature conditions
 806

Primary Model	Secondary model	Solution method	Validation conditions	Reference
and Roberts aranyi and (4).	Quadratic polynomial model.	Numerical solution by the fourth order Runge–Kutta method.	Rates of change of T ranging from 1.7°C.h ⁻¹ to a virtually instantaneous change: cooling from 25°C to -2, 2, 5 or 10°C and heating from 2°C to 25°C.	Bovill et al., 2004
Logistic model.	Arrhenius equation.	Numerical solution by the fourth order Runge–Kutta method.	Various types of a dynamic temperature history with various intervals were studied for of <i>Escherichia coli</i> 1952 growth prediction.	Fujikawa et al., 2004
and Roberts aranyi and (4).	A modified Ratkowsky equation (Zwietering et al., 1991).	Numerical solution by the fourth order Runge–Kutta method.	Growth of <i>Salmonella Enteritidis</i> in egg yolk under varying temperature profiles (exponential and linear cooling, exponential heating and sinusoidal temperatures).	Gumbo et al., 2004
form of the odel (Gibson	A modified Ratkowsky equation (Zwietering et al., 1991).	Numerical solution by the fourth order Runge–Kutta method.	Growth of <i>Clostridium perfringens</i> in cooked ground beef under fluctuating temperature conditions between 30°C and 45°C (square waved) and under continuous temperature changes from 51°C to 10°C (linear and exponential cooling).	Huang et al., 2004

807 Table 2

808 Tested temperature scenarios for the validation of the model at changing air temperature and

809 constant convective heat transfer coefficient equals to $8 \text{ W}/(\text{m}^2 \cdot \text{K})$

810

Stage of the cycle	Temperature (°C)	Duration (h)
Cycle N° 1		
Storage in a cold room	2.5	24
Refrigeration stopped due to an accidental failure of the installation	21	24
Repaired breakdown and remaining product in the cold room	2.5	24
Cycle N° 2		
Industrial storage and transport	9.5	18
Household doorstep delivery	30	4
Storage in refrigerator	9.5	24
Product on the table	30	2
Remaining product in the refrigerator	9.5	18
Cycle N° 3		
Storage and transport	5	24
Storage in the refrigerated cabinet	12	24
Household doorstep delivery	25	4
Storage in refrigerator	8	24

811 Table 3
812 Statistical criteria related to the data of validation at constant air temperature and changing
813 convective heat transfer coefficient
814

Test conditions	R	B_f	A_f
Case 1	0.996	0.98	1.03
Case 2	0.996	0.99	1.01
Case 3	0.987	0.98	1.04
at product centre			
Case 3	0.987	0.99	1.02
at product surface			
Case 4	0.976	0.99	1.05
at product centre			
Case 4	0.986	0.99	1.03
at product surface			
Case 5	0.975	0.99	1.03
at product centre			
Case 5	0.994	1	1.01
at product surface			

815

816
817
818
819
820

Table 4
Statistical criteria related to the data of validation at changing air temperature and constant convective heat transfer coefficient equals to 8 W/(m².K)

Test conditions	<i>R</i>	<i>B_f</i>	<i>A_f</i>
Cycle 1 at product centre	0.991	1.05	1.05
Cycle 1 at product surface	0.992	1.04	1.05
Cycle 2 at product centre	0.963	1.08	1.08
Cycle 2 at product surface	0.986	1.06	1.06
Cycle 3 at product centre	0.944	1.13	1.13
Cycle 3 at product surface	0.964	1.09	1.09

821
822
823